First-principles approach to the electron transport and applications for devices based on carbon nanotubes and ultrathin oxides

Yong-Ju Kang [a], Joongoo Kang [a], Yong-Hoon Kim [b,c], Kee Joo Chang [a,*]

[a] *Department of Physics, Korea Advanced Institute of Science and Technology, Daejeon 305-701, Republic of Korea*
[b] *Korea Institute for Advanced Study, Dongdaemun-gu, Seoul 130-722, Republic of Korea*
[c] *Department of Materials Science and Engineering, University of Seoul, Dongdaemun-gu, Seoul 130-743, Republic of Korea*

Abstract

We use a first-principles computational scheme to study the transport properties of devices based on telescoping carbon nanotubes. The transmission function is calculated through the matrix Green's function method using a Gaussian basis set. Varying the overlap region of the two nanotubes, we compare the effect of interwall interactions on the transport characteriscs with that obtained from a simple tight-binding model. The leakage current through ultrathin gate oxides is also studied for various Si/SiO_2 interface models, which are manipulated by varying oxide thickness and crystal phase.

Key words: quantum transport; matrix Green's function

1. Introduction

One of the major subjects in nanoelectronics is understanding the current-voltage response of an electronic circuit in which molecules or thin films between two electrodes act as conducting elements. Among one-dimensional nanostructures, carbon nanotubes and nanowires have attracted much attention because of a variety of potential applications for nanoscale devices. Single-walled carbon nanotubes are considered as a defect-free system with ballistic conduction, and display zero-bias anomalies with the characteristics of the Luttinger-liquid state [1–3]. The transport behavior of multiwall carbon nanotubes is quite controversial, because a variety of transport mechanisms were observed from ballistic transport, Luttinger-like zero-bias anomalies to diffusive transport, and also strong localization [4–6]. On the other hand, it is projected that the Si-based complementary metal-oxide semiconductor (CMOS) technology will reach absolute limits on its performance within a next decade [7,8]. As the size of CMOS devices is scaled down to the sub-10-nm regime, quantum effects start to become important. Then, the thickness of SiO_2 insulating layers will be in the range of 1-2 nm, and gate leakage current is unavoidable due to direct tunneling of electrons. The non-equilibrium Green's function (NEGF) theory is now widely used for studying at the atomic level the quantum transport of electrons in nanoscale devices [9,10].

In this work we use the matrix Green's function (MGF) approach to calculate the transmission function in devices based on telescoping carbon nanotubes and ultrathin SiO_2 layers. Our calculations are based on the local-density-functional approximation (LDA), with use of a Gaussian basis set of localized orbitals. The surface Green functions for electrodes are obtained iteratively from two separate calculations for bulks, and the self-energies between

* Corresponding author.
Email address: kchang@kaist.ac.kr (Kee Joo Chang).

the device and electrodes are given in the ab-inito fashion. In this scheme, the two-dimensional periodicity of monolayer devices and the semi-infinite nature of electrodes are treated in a consistent and accurate manner by the reciprocal-space k-point sampling. The details of our calculational method are given elsewhere [11].

2. Method

The NEGF theory is a well-developed formalism to treat various non-equlibrium charge transport phenomena. As the matrix version of the NEGF theory, the MGF approach provides a very efficient way to treat the open boundary problem within the linear combination of atomic orbitals (LCAO) formalism [9,10]. We construct a device by sandwiching a molecular monolayer (M) between two semi-infinite electrodes 1 and 2 [11]. For each $\mathbf{k}_\parallel$ point in the two-dimensional reciprocal lattice of molecular monolayer, the LDA Hamiltonian matrix H is partitioned into the LCAO blocks belonging electodes 1 and 2 and the molecule,

$$H = \begin{pmatrix} H_1^{\mathbf{k}_\parallel} & {H_{M1}^{\mathbf{k}_\parallel}}^\dagger & 0 \\ H_{M1}^{\mathbf{k}_\parallel} & H_1^{\mathbf{k}_\parallel} & H_{M2}^{\mathbf{k}_\parallel} \\ 0 & {H_{M2}^{\mathbf{k}_\parallel}}^\dagger & H_2^{\mathbf{k}_\parallel} \end{pmatrix}. \quad (1)$$

Partitioning the overlap matrix S in the same manner, the retarded Green's function in the matrix form is written as,

$$G^{\mathbf{k}_\parallel} = \begin{pmatrix} \varepsilon S_1^{\mathbf{k}_\parallel} - H_1^{\mathbf{k}_\parallel} & {X_1^{\mathbf{k}_\parallel}}^\dagger & 0 \\ X_1^{\mathbf{k}_\parallel} & \varepsilon S_M^{\mathbf{k}_\parallel} - H_M^{\mathbf{k}_\parallel} & X_2^{\mathbf{k}_\parallel} \\ 0 & {X_2^{\mathbf{k}_\parallel}}^\dagger & \varepsilon S_2^{\mathbf{k}_\parallel} - H_2^{\mathbf{k}_\parallel} \end{pmatrix}^{-1} \quad (2)$$

where $X_a = \varepsilon S_{Ma}^{\mathbf{k}_\parallel} - H_{Ma}^{\mathbf{k}_\parallel}$. Then, the molecule part of G is obtained as

$$G_M^{\mathbf{k}_\parallel} = (ES_M^{\mathbf{k}_\parallel} - H_M^{\mathbf{k}_\parallel} - \Sigma_1^{\mathbf{k}_\parallel} - \Sigma_2^{\mathbf{k}_\parallel})^{-1}. \quad (3)$$

Here Σ_a is the self-energy matrix

$$\Sigma_a^{\mathbf{k}_\parallel} = X_a^{\mathbf{k}_\parallel} G_a^{\mathbf{k}_\parallel} {X_a^{\mathbf{k}_\parallel}}^\dagger (a = 1, 2), \quad (4)$$

while the broadening of molecular energy levels is described by the anti-Hermitian part

$$\Gamma_a^{\mathbf{k}_\parallel} = i(\Sigma_a^{\mathbf{k}_\parallel} - {\Sigma_a^{\mathbf{k}_\parallel}}^\dagger). \quad (5)$$

The total transmission is obtained by integrating $T^{\mathbf{k}_\parallel}$ over the 2D reciprocal primitive cell $\widetilde{\Omega}$,

$$T(E) = \frac{1}{\Omega} \int_{\widetilde{\Omega}} d\mathbf{k}_\parallel T^{\mathbf{k}_\parallel}(E), \quad (6)$$

where $T^{\mathbf{k}_\parallel}(E) = Tr(\Gamma_1^{\mathbf{k}_\parallel} G_M^{\mathbf{k}_\parallel} \Gamma_2^{\mathbf{k}_\parallel} {G_M^{\mathbf{k}_\parallel}}^\dagger)$.

From the semi-infinite function $G_a^{\mathbf{k}_\parallel}$, we extract the surface Green's function $g_{Sa}^{\mathbf{k}_\parallel}$ of a finite dimension through three-dimensional bulk calculations for each electrode. Since the same surface Green's function can be obtained by removing one layer of the contact lattice, $G_a^{\mathbf{k}_\parallel}$ satisfies the relation,

$$G_2^{\mathbf{k}_\parallel} = (\varepsilon S_2^{\mathbf{k}_\parallel} - H_2^{\mathbf{k}_\parallel})^{-1} = \begin{pmatrix} g_{S2}^{\mathbf{k}_\parallel} & & \cdots \\ & g_{S2}^{\mathbf{k}_\parallel} & \\ & & g_{S2}^{\mathbf{k}_\parallel} \\ \vdots & & \ddots \end{pmatrix}^{-1}, \quad (7)$$

where each g_{Sa} corresponds to the electrode unit cell. After carrying out 1D Fourier transform of H and S and using a large bulk cell, we obtain the recursion relation for the surface Green's function matrix,

$$g_2^{\mathbf{k}_\parallel} = (\alpha_2^{\mathbf{k}_\parallel} - \beta_2^{\mathbf{k}_\parallel} g_2^{\mathbf{k}_\parallel} {\beta_2^{\mathbf{k}_\parallel}}^\dagger)^{-1}, \quad (8)$$

where

$$\alpha_2^{\mathbf{k}_\parallel} = \varepsilon S_2^{(\mathbf{k}_\parallel, T_0)} - H_2^{(\mathbf{k}_\parallel, T_0)}, \quad (9)$$

$$\beta_2^{\mathbf{k}_\parallel} = \varepsilon S_2^{(\mathbf{k}_\parallel, T_1)} - H_2^{(\mathbf{k}_\parallel, T_1)} \quad (10)$$

and T_m is the surface-normal direction lattice vector of layer m. The characteristics of conducting channels can be analyzed by the projected density of states

$$DOS(E) = \frac{1}{2\pi\Omega} \int_{\widetilde{\Omega}} d\mathbf{k}_\parallel Tr[A_M^{\mathbf{k}_\parallel}(E) S_M^{\mathbf{k}_\parallel}] \quad (11)$$

where $A = i(G - G^\dagger)$ is the spectral function.

3. Results and discussion

Recent experiments have demonstrated that telescopically aligned carbon nanotubes can be obtained by manipulating the core shells of multiwall carbon nanotubes due to low frictions between the walls [12]. As the inner core tubes are pulled out from the

outer tubes, electrical resistance was shown to increase with an exponential form for the extension range of 0.5 - 3 μm, which was attibuted to the localization of electrons [13]. For short telescoping distances, which are defined as the overp region between the inner and outer tubes, electrical conduction will reply on the quantum transport of electrons because scatterings by impurities and defects are not expected. In this case, multiband tight-binding calculations showed that the transmission depends on the chirality, diameter, and composition of nanotubes [14]. However, there is some controversy regarding the quantum conductance of armchair telescoping nanotubes. Especially, in the (5,5)/(10,10) telescoping tube, the maximum conductance was calculated to be less than G_0 or close to $2G_0$, depending on the the tight-binding model, where $G_0 = 2e^2/h$ [14–16]. The discrepancy between the calculations may be attributed to different descriptions of interwall interactions. Since the tight-binding model has limits in describing interwall interactions in multiwall nanotubes, it needs a more accurate approach based on first-principles calculations.

For the (5,5)/(10,10) double-wall nanotubes, we investigate the band structure using the first-principles approach within the LDA, and find that interwall interactions are severely enhanced in the simple π-orbital tight-binding model. Similar to double-wall nanotubes, the transmission of telescoping nanotubes will be strongly affected by the interwall coupling. For the (5,5)/(10,10) telescoping tubes [see Fig. 1(a)], we test telescoping distances up to about 70 Å and various rotational angles which break mirror symmetries, and find that the maximum conductance is less than G_0, in good agreement with the results obtained from the multiband tight-binding calculations [14]. Although the transmission follows the oscillating behavior with increasing the telescoping distance, it does not reach the value of $2G_0$, in contrast to other π-orbital tight-binding calculations [15,16]. When the interwall coupling is weakened in the tight-binding model, the transmission is generally reduced. However, even if the interwall coupling is reduced by 50 %, the maximum conductance is still above G_0. This result indicates that the tight-binding model overestimates the interwall coupling, compared with the LDA calculations.

In Fig. 1(b), the transmission and the local density of states (LDOS) are plotted as a function of energy for the telescoping distance of 39 Å, which exhibits the maximum conductance of about G_0. In the (5,5) and (10,10) nanotubes, the linear bands are almost parallel, thus, the two group velocities at the wave vectors of the two π bands with the energy E are very similar. The period of antiresonances agrees well with the value estimated from these two group velocities. Analyzing the LDOS, we find that the π channel gives rise to the peaks in transmission, while the π^* channel is suppressed. At the transmission peaks, electrons are delocalized, extending into the electrodes. On the other hand, electrons at the dips are found to be localized as a quai-bound state, suppressing the conduction.

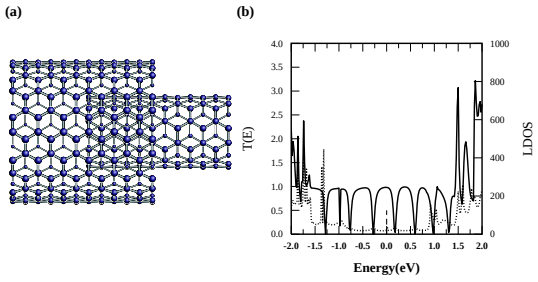

Fig. 1. (a) Atomic structure of the (5,5)/(10,10) telescoping carbon nanotube and (b) the calculated total transmission (solid line) and the local density of states (dotted line).

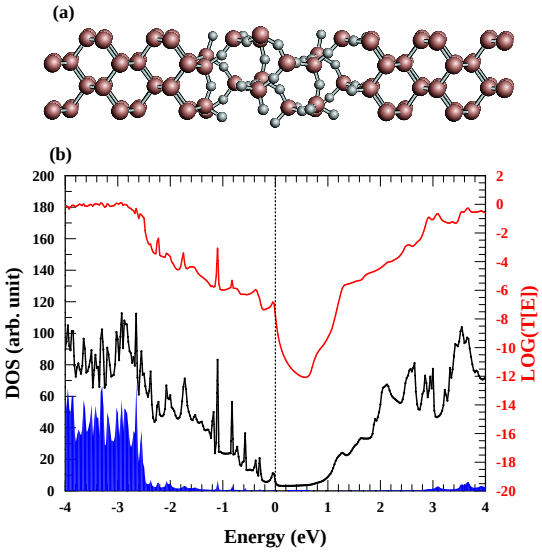

Fig. 2. (a) Atomic structure of the oxide device, where α-quartz SiO_2 is sandwiched between two Si(100) electrodes, and (b) the total transmission (upper curve) and the density of states (lower curve). The shaded area represents the DOS projected onto the oxide region.

Next we examine the direct electron tunneling through ultrathin SiO_2 layers, with different thicknesses and structural phases. We construct several oxide layers based on α-quartz, tridymite, and amorphous structures. One example of the devices used here is drawn in Fig. 2(b), where thin α-quartz SiO_2 is sandwiched between the Si(100) electrodes. The calculated transmission and the DOS are given in Fig. 2(b). We note that the transmission and the projected DOS onto the oxide exhibit very similar behavior in the gap region of SiO_2, which lies between -2.5 and 3.0 eV. This similarity is attributed to the fact that small electron charges from the Si electrodes penetrate into the oxide near the interfaces. On the other hand, the transmission is severely suppressed for energies in the Si band gap, with the top of the valence band set to zero, because there are no states. As the oxide thickness decreases, the tunneling of incident electrons through the penetrated Si states in the oxide region are enhanced. Thus, the transmission tends to increase, almost independent of the oxide structure, enhancing the leakage current owing to the quantum tunneling.

4. Summary

We have performed the first-principles calculations for the transmission function in devices based on telescoping carbon nanotubes and ultrathin SiO_2 oxides, using the matrix Green's function approach. Since there is no scattering by defects, the electrical conduction in these devices will be governed by the quantum transport. Due to the effect of interwall interactions, the transmission of the (5,5)/(10,10) telescoping nanotube depends on the overlap distance of the two tubes. Although the individual tubes have two conducting channels at the Fermi level, only one channel gives rise to the electrical conduction in the telescoping tube, while the other channel is blocked. Thus, the maximum conductance is estimated to be close G_0, in contrast to previous single π-orbital tight-binding calculations, which predicted the maximum conductance close to $2G_0$. Our first-principles calculations indicate that the tight-binding model significantly overestimates the interwall coupling. For thin oxides sandwiched between two Si electrodes, we find that the transmission increases with decreasing the oxide thickness due to the enhanced quantum tunneling.

Acknowledgements

This work was supported by the Korea Ministry of Commerce, Industry and Energy and by the Star-Faculty project.

References

[1] S.J. Tans et al., Nature (London) 393 (1998) 49.

[2] A. Bachtold, M.S. Fuhrer, S. Plyasunov, M. Forero, E.H. Anderson, A. Zettl, P. L. McEuen, Phys. Rev. Lett. 84 (2000) 6082.

[3] A. Javey, J. Guo, Q. Wang, M. Lundstrom, H. Dai, Nature (London) 424 (2003) 654.

[4] A. Bachtold, C. Strunk, J.-P. Salvetat, J.-M. Bonard, L. Forró, T. Nussbaumer, C. Schönenberger, Nature (London) 397 (1999) 673.

[5] S. Frank, P. Poncharal, Z.L. Wang, W.A. de Heer, Science 280 (1999) 1744.

[6] A. Kanda, K. Tsukagoshi, Y. Aoyagi, Y. Ootuka, Phys. Rev. Lett. 92 (2004) 036801.

[7] M. Schulz, Nature (London) 399 (1999) 729.

[8] M. Ieong, B. Doris, J. Kedzierski, K. Rim, M. Yang, Science 306 (2004) 2057.

[9] S. Datta, Electronic transport in mesoscopic systems, Cambridge University Press, Cambridge, 1995; Nanotechnology 15 (2004) S433.

[10] H. Haug and A.-P. Jahuo, Quantum kinetics in transport and optics of semiconductors, Springer, Berlin, 1996.

[11] Y.-H. Kim, J. Tahir-Kheli, P.A. Schultz, W.A. Goddard III, Phys. Rev. B 73 (2006) 235419.

[12] J. Cumings, A. Zettl, Science 289 (2000) 602.

[13] J. Cumings, A. Zettl, Phys. Rev. Lett. 93 (2004) 086801.

[14] D.-H. Kim, K.J. Chang, Phys. Rev. B 66 (2002) 155402.

[15] C. Buia, A. Buldum, J.P. Lu, Phys. Rev. B 67 (2003) 113409.

[16] R. Tamura, Y. Sawai, J. Haruyama, Phys. Rev. B 72 (2005) 045413.